Trans. of the Society of Instrument and Control Engineers
Vol.E-5, No.1, 35/44 (2006)

Performance Analysis of a Recursive Maximum Filter

Ken'ichi Nishiguchi*

A recursive maximum filter (RMF) is an algorithm devised to solve the problem of detecting small moving targets in noisy image sequences. The RMF algorithm is simple and effective for enhancing small moving targets with a low signal-to-noise ratio; however, its principle and performance limit are not clear because it is derived heuristically. In this paper, we reformulate RMF based on Bayes estimation and show that it can be interpreted as a Bellman equation of dynamic programming (DP). Although some DP-based algorithms have already been proposed, RMF requires much less computation than previous algorithms because its state space is much smaller. RMF includes two design parameters: neighborhood size and a forgetting factor. We derive approximation formulae of the distributions of RMF outputs for various parameter values. By using the formulae, we show a minimum SNR with which targets are detectable for each neighborhood size. We also show the conditions under which targets can be detected by RMF with various parameter values.

Key Words: image processing, small target detection, recursive filter, dynamic programming, performance analysis

1. Introduction

Recently, the problem of detecting small targets with low contrast from noisy image sequences has attracted much attention [1)~9)]. This problem arises, for instance, when detecting far moving targets from an onboard infrared (IR) camera [1)] and detecting meteors and artificial satellites in the night sky from a telescope and a charge-coupled device (CCD) [2)]. The problem's difficulty is that objects to be detected (targets) cannot be detected from each single image since they are small with low signal-to-noise ratio (SNR), which cannot be improved by lengthening the integration time since the targets move.

Various methods have been proposed to solve the problem of small target detection. In the research's early stage, assuming that the velocity of the targets is known, a maximum likelihood method [2)] and a three-dimensional matched filter [3),4)] were proposed. The performance of these methods is degraded when the velocity disagrees with the assumed one or when targets maneuver.

Afterwards, on the assumption that the velocities of targets are constant but unknown, methods based on dynamic programming (DP) have been proposed [1),5)]. These DP-based methods can prevent performance degradation due to velocity disagreement since they estimate targets' velocity and can deal with low-maneuvering targets. Furthermore, the performance of DP-based methods was analyzed using false alarm and detection probabilities [6)~8)]. However, since the computational burden on the methods that estimate target velocities is huge, real-time processing is difficult. In addition, constant velocity assumption is too restrictive in applications since apparent random motions caused by camera vibration may be added to the actual target's motion.

We proposed an image processing algorithm called recursive max filter or recursive maximum filter (RMF) [9)] to overcome these difficulties. This algorithm was applied to the detection of small moving targets from an infrared image sequence [9)] and dim star detection from star sensor images [10),11)]. In these applications, the detection performance was validated by simulations using generated and field data. However, since the RMF algorithm was derived heuristically, its principle and its detection performance limit were not clear. In this paper, we interpret RMF from the viewpoint of Bayesian estimation and clarify its target detection performance by analysis and simulation.

The target motion model in this paper is Brownian motion in an image plane. A posteriori probability of the target's trajectory is obtained by applying Bayes' rule to an image sequence that includes both targets and noise. Although a large-scale combinatorial optimization problem must be solved to obtain the optimal trajectory that maximizes the a posteriori probability, the exact solution is easily determined with a dynamic programming (DP) approach. We show that the Bellman equation of DP for this problem becomes the recursive formula of RMF.

In addition, we derive an approximate distribution of RMF's output with which we evaluate its performance.

* Advanced Technology R&D Center, Mitsubishi Electric Corporation, Amagasaki (then)
Frontier Research Center, Osaka University, Suita (now)

Output SNR can be increased indefinitely if input SNR exceeds a certain value, which is referred to as limit SNR. We obtain the values of the limit SNR . Moreover, we clarify the conditions under which targets are detectable in various situations.

The organization of this paper is as follows. In Section 2, RMF is interpreted from the viewpoint of Bayesian estimation. In Section 3, the distribution of RMF output image intensities is obtained, which is necessary for performance analysis. In Section 4, limit SNR and the SNR improvement effect of RMF are discussed. In Section 5, the false alarm and detection probabilities by RMF are obtained. Finally, Section 6 draws some conclusions.

2. Recursive maximum filter

2.1 Model of small target detection

Let $Y_{ij}(k), i,j = 1,\cdots,n, k = 1,2,\cdots$ be the image sequences to be processed, where (i,j) denotes the pixel number and k the frame number at time t_k. The image data contain targets, a structured background, clutter, and noise. Except for the noise, here we assume that the backgrounds are negligible or have already been whitened by preprocessing. We assume that the targets move randomly from frame to frame. This assumption does not exclude the possibility of constant velocity movement, but implies a lack of knowledge about the motion of targets. We also assume that the maximum velocity of a target is known, which is denoted by $v_{\max}$. For pixel (i,j), we define neighborhood D_{ij} as a region where the target, which is present at pixel (i,j) in one image, may have existed in the preceding image. Let ν be the number of pixels contained in D_{ij}. Here D_{ij} and ν are determined by the maximum velocity of the targets. For example, when $v_{\max} \leq 1$ pixels/frame, D_{ij} is given by

$$D_{ij} = \{(i',j')\,;\ i' = i, i \pm 1,\ j' = j, j \pm 1\}, \tag{1}$$

and $\nu = 9$.

We assume that background noise $W_{ij}(k)$ is Gaussian with a mean of μ and a variance of σ^2, and it is white both in time and space, i.e.:

$$E(W_{ij}(k)) = \mu, \tag{2}$$

$$E((W_{ij}(k)-\mu)(W_{i'j'}(k')-\mu)) = \sigma^2\,\delta_{ii'}\,\delta_{jj'}\,\delta_{kk'}, \tag{3}$$

where $E(\cdot)$ denotes the expectation and $\delta_{ii'}$ is Kronecker's delta.

Let A be the intensity of a target. Then the image data are represented as

$$Y_{ij}(k) = \begin{cases} A + W_{ij}(k), & \text{if a target is present} \\ W_{ij}(k), & \text{otherwise} \end{cases} \tag{4}$$

We define the input SNR of a target as

$$\mathrm{SNR_{in}} = \frac{A-\mu}{\sigma}. \tag{5}$$

If we detect targets in a single frame of image data by thresholding, then $\mathrm{SNR_{in}}$ must be greater than 6 or 7. The problem treated in this paper is the detection of targets that cannot be detected in a single frame of image data. Therefore, the $\mathrm{SNR_{in}}$ value we are concerned with is less than 2 or 3.

2.2 RMF algorithm

If a target is present at location (i,j) at time k, then it must have been in neighborhood D_{ij} at time $k-1$, so quantity $Y_{ij}(k) + \max_{(i',j')\in D_{ij}} Y_{i'j'}(k-1)$ is expected to take a larger value than in the case of no targets. If the target is assumed to have been at location (i',j') at time $k-1$, then it must have been in neighborhood $D_{i'j'}$ at time $k-2$, so quantity $Y_{ij}(k) + \max_{(i',j')\in D_{ij}}\{Y_{i',j'}(k-1) + \max_{(i'',j'')\in D_{i'j'}}\{Y_{i'',j''}(k-2)\}\}$ is expected to take a much larger value and so on. Thus the summation of the maximum value of the neighborhood back to its former location

$$X_{ij}(k) = Y_{ij}(k) + \max_{(i',j')\in D_{ij}} \Biggl\{ Y_{i'j'}(k-1) + \max_{(i'',j'')\in D_{i'j'}} \{Y_{i''j''}(k-2) + \cdots\} \Biggr\} \tag{6}$$

can be expected to take a large value when the target is present at location (i,j). On the other hand, when targets are absent, the above quantity is the summation of temporally uncorrelated noise. As a result, it is expected to take a relatively small value. Therefore the quantity behaves to enhance the moving targets and suppress noise. $X_{ij}(k)$ can be calculated by the recursive algorithm as

$$X_{ij}(k) = Y_{ij}(k) + \max_{(i',j')\in D_{ij}} X_{i'j'}(k-1), \quad k = 1,2,\cdots \tag{7}$$

where we set $X_{ij}(0) = 0$. The above algorithm, however, has drawbacks. First, the recursive procedure corresponds to putting equal weights on all the past data while it is desirable to put additional weight on the later data. Second, since $X_{ij}(k)$ becomes larger and larger with time, resetting $X_{ij}(k)$ is required while temporally homogeneous processing is preferable because the time of the appearance of the targets is not known. To avoid such drawbacks, we modify algorithm (7) using a forgetting factor α as

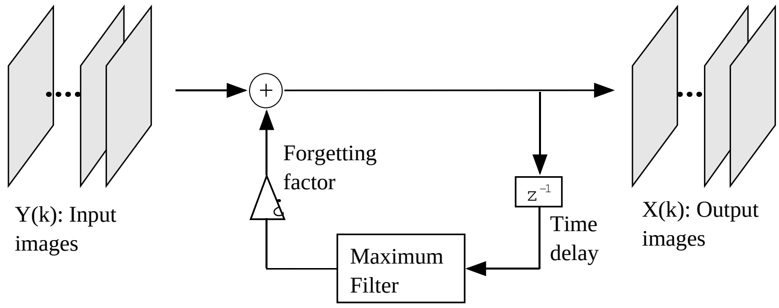

Fig. 1 Block diagram of recursive maximum filter

$$X_{ij}(k) = Y_{ij}(k) + \alpha \max_{(i',j')\in D_{ij}} X_{i'j'}(k-1), \quad k = 1, 2, \cdots \tag{8}$$

which we call the recursive max filter (RMF)[9]. The closer the value of α is to one, the greater the integration effect; however when α equals one, RMF will diverge as time goes on. Therefore, we set the value of α less than one (for example, 0.9 or 0.95) for the persistent use of RMF in such cases to await the appearance of targets. On the contrary, if RMF is reset at fixed intervals, we set $\alpha = 1$.

The algorithm of (8) can be implemented by the architecture shown in **Fig. 1**. The RMF in Fig. 1 has a local maximum filter in its loop. Targets are enhanced by RMF with elapsed time and detected by thresholding with an adequate threshold; even though RMF is very simple, it detects dim moving targets well.

2.3 RMF formulation by Bayesian estimation and DP

Although RMF was originally derived in a heuristic manner, as stated in the preceding section, the problem can be formulated as a Bayesian estimation problem and the RMF algorithm can be derived as a Bellman equation of DP. In this section, we derive RMF in such a manner.

Let $\phi(k) = (i_k, j_k)$ be the pixel where a target exists at time k, and $\phi^k = (\phi(1), \cdots, \phi(k))$ be the target's trajectory to time k. When image data to time k, $Y^k = (\{Y_{ij}(1)\}, \cdots, \{Y_{ij}(k)\})$ are given, let $P(\phi^k \mid Y^k)$ be the a posteriori probability of target trajectory ϕ^k. By Bayes' rule this probability is represented as

$$P(\phi^k \mid Y^k) = \frac{P(Y^k \mid \phi^k)P(\phi^k)}{P(Y^k)}, \tag{9}$$

where $P(\phi^k)$ is the a priori probability of target trajectory, and by the assumption that target's motion is random it is represented as

$$P(\phi^k) = P(\phi(1)) \prod_{l=2}^{k} P(\phi(l) \mid \phi(l-1)). \tag{10}$$

The initial distribution is $P(\phi(1)) = 1/N^2$ since all pixels are equally likely, and the transition probability is nonzero only when $\phi(l-1)$ is included in the neighborhood of $\phi(l)$ by definition of the neighborhood, i.e.:

$$P(\phi(l) \mid \phi(l-1)) = \begin{cases} 1/\nu, & \text{if } \phi(l-1) \in D_{\phi(l)}, \\ 0, & \text{otherwise.} \end{cases} \tag{11}$$

Consequently, $P(\phi^k)$ takes the same value of $1/\nu^{k-1}N^2$ on possible trajectories and zero otherwise. Conditional probability $P(Y^k \mid \phi^k)$ on the right-hand side of (9) is the probability density of observed values given a target trajectory. Since the observation noise is white both in time and space, it is represented as

$$P(Y^k \mid \phi^k) = \prod_{l=1}^{k} \prod_{i,j=1}^{N} p(Y_{ij}(l) \mid \phi(l)). \tag{12}$$

Since each term on the right-hand side is given by

$$p(Y_{ij}(l) \mid \phi(l)) = \frac{1}{\sqrt{2\pi\sigma^2}} \times \begin{cases} \exp\left[-\dfrac{(Y_{ij}(l) - \mu - A)^2}{2\sigma^2}\right], & (i,j) = \phi(l) \\ \exp\left[-\dfrac{(Y_{ij}(l) - \mu)^2}{2\sigma^2}\right], & (i,j) \neq \phi(l) \end{cases} \tag{13}$$

we obtain

$$P(Y^k \mid \phi^k) = M_1 \prod_{l=1}^{k} \exp\left\{-\frac{1}{2\sigma^2}\left[-2A(Y_{\phi(l)}(l) - \mu) + A^2\right]\right\}, \tag{14}$$

which is substituted into (9) to get

$$P(\phi^k \mid Y^k) = M_2 P(\phi^k) \times \exp\left\{-\frac{1}{2\sigma^2}\sum_{l=1}^{k}\left[-2A(Y_{\phi(l)}(l) - \mu) + A^2\right]\right\}, \tag{15}$$

where M_1 and M_2 are constants that do not depend on the target trajectory. The maximization of (15) with respect to ϕ^k is equivalent to maximizing

$$J(k) = P(\phi^k)\sum_{l=1}^{k} Y_{\phi(l)}(l), \tag{16}$$

regardless of the value of A. So far, we have considered the problem on the basis that targets exist from the outset; however, there are applications where targets are absent at the outset but we want to detect them as rapidly as possible after their appearance. Therefore, we introduce an object function defined by

$$J(k) = P(\phi^k)\sum_{l=1}^{k} \alpha^{k-l} Y_{\phi(l)}(l), \tag{17}$$

where α $(0 < \alpha \le 1)$ is the forgetting factor introduced in the preceding section.

The goal is to obtain a trajectory that maximizes object function $J(k)$ among all possible trajectories. This becomes an extremely large-scale combinatorial optimization problem in which the number of trajectories is $\nu^{k-1}N^2$; for example, if $\nu = 7 \times 7$, $k = 30$ and $N = 512$, then the number of trajectories is 2.7×10^{54}. However, in this case we can effectively obtain the exact solution with DP.

We introduce function $X_{ij}(k)$ defined by

$$X_{ij}(k) = \max_{\phi^k;\phi(k)=(i,j)} \nu^{k-1}N^2 J(k), \tag{18}$$

and then it holds

$$\max_{\phi^k} \nu^{k-1}N^2 J(k) = \max_{i,j} X_{ij}(k), \tag{19}$$

so that the maximization of $J(k)$ with respect to all trajectories is equivalent to maximizing $X_{ij}(k)$ with respect to i and j.

Note that the object function can be written in the following recursive form:

$$\begin{aligned} J(k) \;&=\; P(\phi^k)Y_{\phi(k)}(k) + \alpha P(\phi(k)\,|\,\phi(k-1))J(k-1), \\ &\qquad k = 1, 2, \cdots \end{aligned} \tag{20}$$

with $J(0) = 0$. By substituting (20) into (18) and using (11) we obtain a Bellman equation with respect to $X_{ij}(k)$ such that

$$\begin{aligned} X_{ij}(k) \;&=\; Y_{ij}(k) + \alpha \max_{\{\phi^{k-1};\phi(k-1)\in D_{ij}\}} J(k-1) \\ &=\; Y_{ij}(k) + \alpha \max_{(i',j')\in D_{ij}} X_{i'j'}(k-1) \end{aligned} \tag{21}$$

with initial value $X_{ij}(0) \equiv 0$, which is exactly the RMF in the preceding section.

In this way, RMF can be interpreted as a DP-based algorithm; however, the amount of calculation is much smaller than by conventional DP-based methods for small target detection. This is because, while the search space of the conventional methods is a set of the trajectories of both positions and velocities, RMF's set only includes the trajectories of positions, enabled by assuming the movable regions of targets. The dominant calculation of RMF is the N^2 operation of the local maximization at each time. Since search space is the product space of the position and velocities in the conventional methods, if the number of cells in the velocity space is M^2, then $N^2 \times M^2$ operations of local maximization are needed. For example, Tonissen et al.[7] and Johnston et al.[8] use 6×6 velocity cells, so the amount of calculation for RMF is reduced 1/36.

3. Distribution of output image intensities of RMF

In this section, we investigate the distribution of the intensities of RMF output images when a target is both absent and present. Without loss of generality, we assume $\mu = 0$ and $\sigma = 1$; otherwise, we may replace $(Y_{ij}(k)-\mu)/\sigma$ by $Y_{ij}(k)$. Under this assumption, the intensity of target A in itself becomes the input SNR.

3.1 Distribution of output noise

Here we refer to RMF output when input images only contain noise as output noise. Although, the distribution of the output noise must be determined to obtain the false alarm probability, determining the distribution exactly is difficult since RMF output includes the maximum of the correlated variables, as seen in (8). So we obtain an approximate distribution.

First, under the assumption that output noise is independent and an identically distributed normal variable in the neighborhood, the mean of output noise $\mu_{\text{out}}(k)$ is approximated by

$$\mu_{\text{out}}(k) \sim \begin{cases} (k-1)\mu_0(\nu,1), & \alpha = 1, \\ \alpha\dfrac{1-\alpha^{k-1}}{1-\alpha}\mu_0(\nu,\alpha), & \alpha < 1, \end{cases} \tag{22}$$

where

$$\mu_0(\nu,\alpha) = \frac{\mu_{(\nu)}}{\sqrt{1-(\alpha\sigma_{(\nu)})^2}} \tag{23}$$

and $\mu_{(\nu)}$ and $\sigma^2_{(\nu)}$ are the mean and the variance of the sample maximum of ν standard normal variables, respectively, which take values shown in **Table 1**[12]. The derivation of (22) is shown in Appendix A. Equation (22) shows that the mean increases linearly when $\alpha = 1$. In **Fig. 2**, both the mean calculated by (22) and the sample mean

Table 1 Means and variances of maximum of standard normal variables

number of variables ν	mean $\mu_{(\nu)}$	variance $\sigma^2_{(\nu)}$
9 ($= 3 \times 3$)	1.485	0.3574
25 ($= 5 \times 5$)	1.965	0.2585
49 ($= 7 \times 7$)	2.241	0.2168
81 ($= 9 \times 9$)	2.431	0.1930

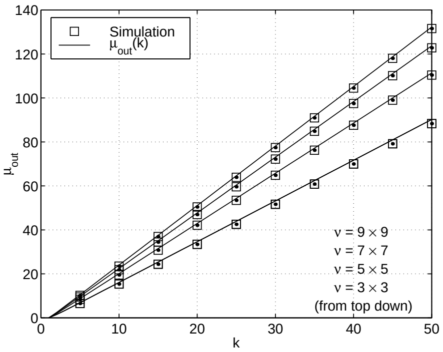

(a) $\alpha = 1$

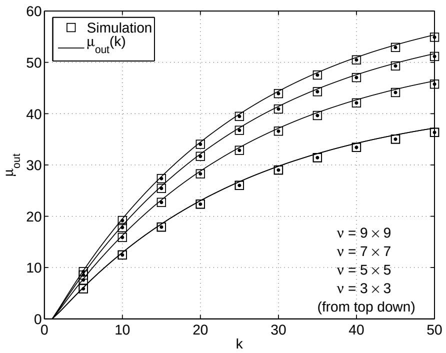

(b) $\alpha = 0.96$

Fig. 2 Mean of output noise

$$\mu_{\mathrm{s}}(k) = \frac{1}{N^2} \sum_{i,j=1}^{N} Z_{ij}(k) \tag{24}$$

are plotted when $\alpha = 1$ and 0.96. Here, the image size in the simulation is $N = 1024$. As is shown in the figure, (22) gives an excellent approximation despite being based on a rough assumption.

Next, we denote the variance of output noise as $\sigma^2_{\mathrm{out}}(k)$. Unlike the mean of output noise, analytically deriving an approximate expression of $\sigma^2_{\mathrm{out}}(k)$ is difficult. This is because such global statistical properties as a long-range correlation affect $\sigma^2_{\mathrm{out}}(k)$, while in the case of $\mu_{\mathrm{out}}(k)$ we may only assume local statistical properties in the neighborhood. For this reason, we derive an approximation expression with the aid of simulation results. We define the local maximum of output noise as

$$Z_{ij}(k) = \max_{(i',j') \in D_{ij}} X_{i'j'}(k). \tag{25}$$

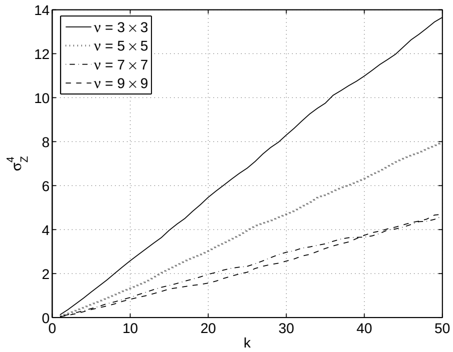

Fig. 3 Square of variance of $Z_{ij}(k)$ (simulation, $\alpha = 1$)

Assuming that the time increments of $Z_{ij}(k)$ are independent, Nishiguchi et al. [9] derived an approximation expression:

$$\begin{aligned} \sigma^2_Z(k) &= (1 + \alpha^2 + \cdots + \alpha^{2(k-1)})\sigma^2_{(\nu)} \\ &= \frac{1 - \alpha^{2k}}{1 - \alpha^2} \sigma^2_{(\nu)}, \end{aligned} \tag{26}$$

from which, when $\alpha = 1$, the variance increases in proportion to time. On the other hand, **Fig. 3** shows the time evolution of the square of $Z_{ij}(k)$'s sample variance, where sample variance is defined by

$$\sigma^2_{\mathrm{s}}(k) = \frac{1}{N^2} \sum_{i,j=1}^{N} (Z_{ij}(k) - \mu_{\mathrm{s}}(k))^2. \tag{27}$$

As shown in the figure, the square of the variance linearly increases instead of the variance itself. This nontrivial property must be clarified theoretically; however, it has been an open problem up to now. Accordingly, we exploit only the property and modify the approximation expression of $Z_{ij}(k)$'s variance as

$$\sigma^2_Z(k) = \begin{cases} \sqrt{k}\sigma^2_0(\nu, 1) & \alpha = 1 \\ \sqrt{\dfrac{1 - \alpha^{2k}}{1 - \alpha^2}} \sigma^2_0(\nu, \alpha), & \alpha < 1 \end{cases} \tag{28}$$

where $\sigma_0(\nu, \alpha)$ is an unknown parameter to be determined by simulation. Here we determined $\sigma_0(\nu, \alpha)$ by fitting $\sigma^2_Z(k)$ of (28) to sample variance $\sigma^2_{\mathrm{s}}(k)$ using a least squares method because the sample variance is approximately normally distributed by the central limit theorem. **Figure 4** shows examples where sample standard deviation $\sigma_{\mathrm{s}}(k)$ is approximated by $\sigma_Z(k)$ of (28). Other than these examples, the approximation is quite good. In **Fig. 5**, we show the values of σ_0, determined by simulation for each α and ν.

Note that when the input is only noise, the recursive formula for RMF can be written as

$$X_{ij}(k) = W_{ij}(k) + \alpha Z_{ij}(k-1), \tag{29}$$

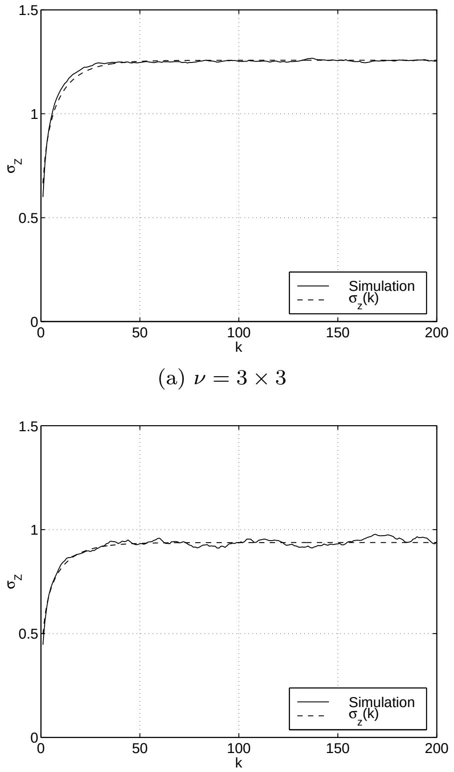

(a) $\nu = 3 \times 3$

(b) $\nu = 9 \times 9$

Fig. 4 Model fitting to standard deviation of $Z_{ij}(k)$ ($\alpha = 0.96$)

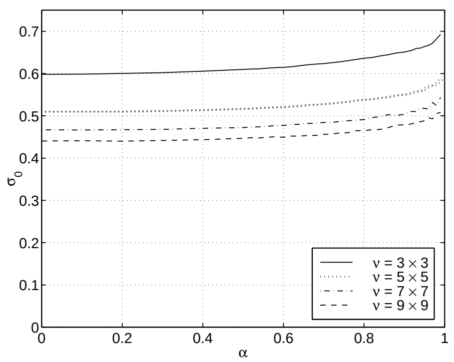

Fig. 5 Estimates of model parameter σ_0

from which the variance of output noise is given by

$$\sigma^2_{\text{out}}(k) = 1 + \alpha^2 \sigma^2_Z(k-1). \tag{30}$$

If $\alpha < 1$, $X_{ij}(k)$ has a stationary state, and the mean and the variance at the stationary state are given by

$$\mu_{\text{out}} = \frac{\alpha \mu_0(\nu, \alpha)}{1-\alpha}, \tag{31}$$

$$\sigma^2_{\text{out}} = 1 + \frac{\alpha^2 \sigma^2_0(\nu, \alpha)}{\sqrt{1-\alpha^2}}. \tag{32}$$

3.2 Output image pixel intensities in the presence of a target

In the input image, the mean and the variance of the intensity of a pixel that contains a target are A and 1, respectively. In the output image, if A is sufficiently large, the pixel intensity that contains a target is considered the sum of pixel intensities returning to the past with forgetting factors along the target trajectory. Since weight α^l is multiplied to the image of l frames ago, the mean and the variance of the element of the sum are $\alpha^l A$ and α^{2l}, respectively. As a result, the mean and the variance of the target pixel intensity are given by

$$\mu_{\text{T}}(k) = \begin{cases} kA, & \alpha = 1 \\ \dfrac{1-\alpha^k}{1-\alpha} A, & \alpha < 1 \end{cases} \tag{33}$$

$$\sigma^2_{\text{T}}(k) = \begin{cases} k, & \alpha = 1 \\ \dfrac{1-\alpha^{2k}}{1-\alpha^2}, & \alpha < 1. \end{cases} \tag{34}$$

In addition, if $\alpha < 1$, there is a stationary state in the RMF, and if it has attained the stationary state when a target appears, then the mean and the variance of the target pixel intensity become

$$\mu_{\text{T}}(k) = \frac{1-\alpha^k}{1-\alpha} A + \alpha^k \mu_{\text{out}}, \tag{35}$$

$$\sigma^2_{\text{T}}(k) = \frac{1-\alpha^{2k}}{1-\alpha^2} + \alpha^{2k} \sigma^2_{\text{out}}. \tag{36}$$

4. Target enhancement by RMF

4.1 Output SNR and limit SNR

RMF has an enhancement effect on low-SNR targets that are buried in noise. We quantitatively evaluate the effect by regarding it as an improvement effect on output SNR. Assuming that RMF is in a stationary state when a target appears, we define the output SNR of RMF by

$$\text{SNR}_{\text{out}}(k) = \frac{\mu_{\text{T}}(k) - \mu_{\text{out}}}{\sigma_{\text{out}}}, \tag{37}$$

into which, substituting (35), (31), and (32), we have

$$\text{SNR}_{\text{out}}(k) = \frac{\dfrac{1-\alpha^k}{1-\alpha}(A - \alpha \mu_0(\nu, \alpha))}{\sqrt{1 + \dfrac{\alpha^2 \sigma^2_0(\nu, \alpha)}{\sqrt{1-\alpha^2}}}}. \tag{38}$$

When $k \to \infty$, it approaches

$$\text{SNR}_{\text{out}}(\infty) = \frac{A - \alpha \mu_0(\nu, \alpha)}{(1-\alpha)\sqrt{1 + \dfrac{\alpha^2 \sigma^2_0(\nu, \alpha)}{\sqrt{1-\alpha^2}}}}. \tag{39}$$

Furthermore, when $\alpha \to 1$, it holds that

$$\text{SNR}_{\text{out}}(\infty) \sim \frac{(2/\pi)^{1/4}}{(1-\alpha)^{3/4}} \frac{A - \mu_0(\nu, 1)}{\sigma_0.(\nu, 1)}. \tag{40}$$

Therefore, if A ($= \text{SNR}_{\text{in}}$) is greater than $\mu_0(\nu, 1)$, SNR_{out} can be increased indefinitely by approaching α to 1. Conversely, if A is less than $\mu_0(\nu, 1)$, the target cannot be enhanced, regardless how many image frames are processed.

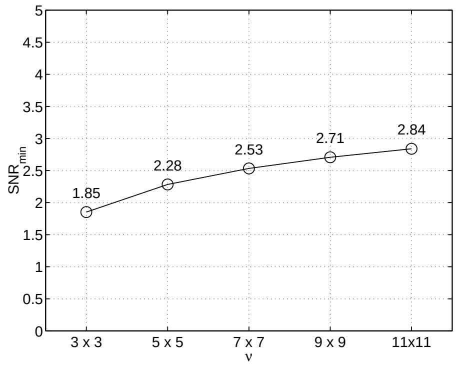

Fig. 6 Limit SNRs

In this sense,

$$\mathrm{SNR}_{\min} \stackrel{\mathrm{def}}{=} \mu_0(\nu, 1) = \frac{\mu_{(\nu)}}{\sqrt{1-\sigma_{(\nu)}^2}} \tag{41}$$

gives a performance limit of the RMF. **Figure 6** shows $\mathrm{SNR}_{\min}$ for each neighborhood size ν. Since $\mathrm{SNR}_{\mathrm{in}}$ must be at least six to detect a target from an image, as stated previously, RMF can reduce it from 1/2 to 1/3.

4.2 SNR improvement effect in the transient state

In the preceding section, we assumed the number of input images is infinite; however, targets must be detected within a finite time. Here, we analyze the growth of output SNR in a transient state.

If we assume that a target is present in the initial state of RMF, then its output SNR is written as

$$\mathrm{SNR}_{\mathrm{out}}(k) = \frac{\mu_{\mathrm{T}}(k) - \mu_{\mathrm{out}}(k)}{\sigma_{\mathrm{out}}(k)}. \tag{42}$$

The values of this $\mathrm{SNR}_{\mathrm{out}}(k)$ calculated by substituting (33), (22), and (30) with $\alpha = 1$ and 0.96 are plotted in **Fig. 7**. This figure shows the SNR improvement effect; if input SNR is greater than $\alpha\mu_0(\nu, \alpha)$, then output SNR increases as k increases. In Fig. 7(d)–(f), the SNR improvement effect is plotted in both cases where RMF has been in stationary and initial states when a target appears. These were calculated by (38). As seen in this figure, the SNR improvement effect does not depend on what states a target appears in but on the number of frames from the appearance of the target.

5. Detection performance of targets

Generally, false alarm and detection probabilities are used to evaluate the performance of target detection algorithms. For each threshold, the detection and false alarm probabilities are defined as the probabilities in which the output exceeds the threshold in the presence and the absence of targets, respectively.

5.1 False alarm probability

For RMF output, we set

$$X_{\max}(k) = \max_{i,j} X_{ij}(k). \tag{43}$$

Let $H(k)$ be the detection threshold of RMF, and then the false alarm probability is represented as

$$P_{\mathrm{FA}} = \Pr(X_{\max}(k) \geq H(k) \,|\, \text{no target}). \tag{44}$$

For clarification, we normalize $X_{\max}$ by the mean and the variance of the RMF output noise as

$$\overline{X}_{\max}(k) = \frac{X_{\max}(k) - \mu_{\mathrm{out}}(k)}{\sigma_{\mathrm{out}}(k)}, \tag{45}$$

and also we normalize the threshold as

$$H(k) = \mu_{\mathrm{out}}(k) + h\sigma_{\mathrm{out}}(k), \tag{46}$$

where h is a threshold parameter. Then, false alarm probability is rewritten as

$$P_{\mathrm{FA}}(h) = \Pr(\overline{X}_{\max}(k) \geq h \,|\, \text{no target}). \tag{47}$$

Since $\overline{X}_{\max}(k)$ is a sample maximum, its distribution is an extremal value distribution that is known as a heavy tail distribution. In addition, $\overline{X}_{\max}(k)$ is regarded as almost a stationary process because it is normalized. In simulation, we calculated 10^5 samples of $\overline{X}_{\max}(k)$ for fixed ν and α and obtained the empirical distribution of false alarm probability (**Fig. 8**). As is seen in this figure, the dependency of the false alarm probability on ν is small. With respect to α, the closer it is to 1, the higher the false alarm probability is. For example, if $0.9 \leq \alpha \leq 0.98$, then it is only necessary to set $h = 7.5$ to keep $P_{\mathrm{FA}} < 10^{-4}$. On the other hand, if X is a standard normal variable, then $\Pr(X \geq 3.72) = 10^{-4}$. This is the consequence of the distribution of $\overline{X}_{\max}(k)$ having a heavy tail.

5.2 Detection probability

Let $X_{\mathrm{T}}(k)$ be the output pixel intensity of RMF in which a target exists. As defined in Section 3.2, its mean and variance are $\mu_{\mathrm{T}}(k)$ and $\sigma_{\mathrm{T}}^2(k)$, respectively. If we assume that $X_{\mathrm{T}}(k)$ follows a normal distribution, its probability density function is written as

$$p_{\mathrm{T}}(x; k) = \frac{1}{\sqrt{2\pi\sigma_{\mathrm{T}}^2(k)}} \exp\left[-\frac{(x-\mu_{\mathrm{T}}(k))^2}{2\sigma_{\mathrm{T}}^2(k)}\right], \tag{48}$$

from which the detection probability for threshold $H(k)$ is given by

$$P_{\mathrm{d}}(k) = \int_{H(k)}^{\infty} \frac{1}{\sqrt{2\pi\sigma_{\mathrm{T}}^2(k)}} \exp\left[-\frac{(x-\mu_{\mathrm{T}}(k))^2}{2\sigma_{\mathrm{T}}^2(k)}\right] dx. \tag{49}$$

We normalize $X_{\mathrm{T}}(k)$ by the mean and the standard deviation of the output noise as

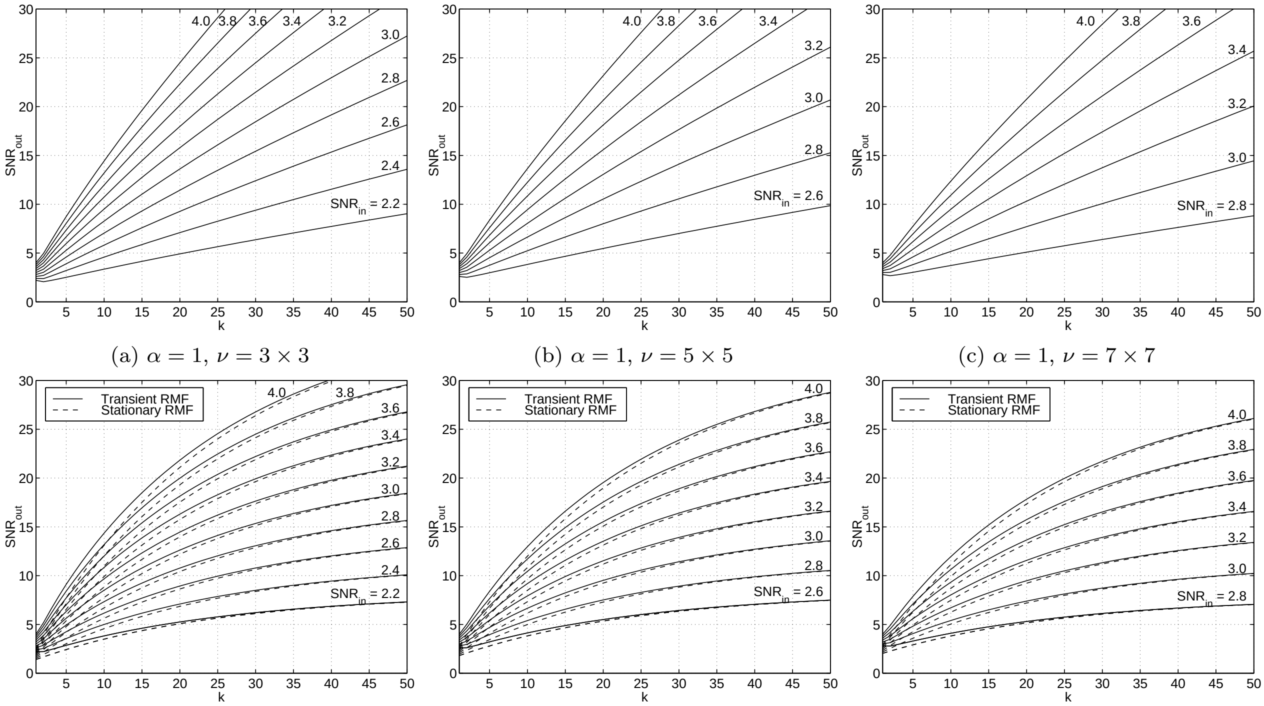

(a) $\alpha = 1$, $\nu = 3 \times 3$ (b) $\alpha = 1$, $\nu = 5 \times 5$ (c) $\alpha = 1$, $\nu = 7 \times 7$

(d) $\alpha = 0.96$, $\nu = 3 \times 3$ (e) $\alpha = 0.96$, $\nu = 5 \times 5$ (f) $\alpha = 0.96$, $\nu = 7 \times 7$

Fig. 7 SNR improvement effect

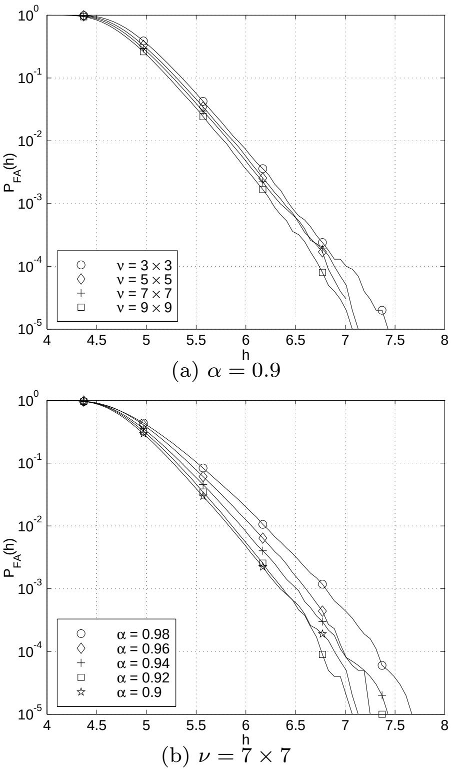

(a) $\alpha = 0.9$

(b) $\nu = 7 \times 7$

Fig. 8 False alarm probability

$$\overline{X}_{\mathrm{T}}(k) = \frac{X_{\mathrm{T}}(k) - \mu_{\mathrm{out}}(k)}{\sigma_{\mathrm{out}}(k)}, \tag{50}$$

whose mean and variance are given respectively by

$$E\overline{X}_{\mathrm{T}}(k) = \frac{\mu_{\mathrm{T}}(k) - \mu_{\mathrm{out}}(k)}{\sigma_{\mathrm{out}}(k)} = \mathrm{SNR}_{\mathrm{out}}(k), \tag{51}$$

$$E(\overline{X}_{\mathrm{T}}(k) - \mathrm{SNR}_{\mathrm{out}}(k))^2 = \left(\frac{\sigma_{\mathrm{T}}(k)}{\sigma_{\mathrm{out}}(k)}\right)^2. \tag{52}$$

Therefore, since the probability density function of $\overline{X}_{\mathrm{T}}(k)$ is given by

$$\begin{aligned}\overline{p}_{\mathrm{T}}(x;k) \;=\; & \frac{1}{\sqrt{2\pi(\sigma_{\mathrm{T}}(k)/\sigma_{\mathrm{out}}(k))^2}} \\ & \times \exp\left[-\frac{(x - \mathrm{SNR}_{\mathrm{out}}(k))^2}{2\sigma_{\mathrm{T}}^2(k)/\sigma_{\mathrm{out}}^2(k)}\right],\end{aligned} \tag{53}$$

the detection probability can be written as:

$$\begin{aligned}P_{\mathrm{d}}(k) \;&=\; \int_h^{\infty} \overline{p}_{\mathrm{T}}(x;k)dx \\ &=\; 1 - \Phi\left(\frac{h - \mathrm{SNR}_{\mathrm{out}}(k)}{\sigma_{\mathrm{T}}(k)/\sigma_{\mathrm{out}}(k)}\right),\end{aligned} \tag{54}$$

where

$$\Phi(x) = \int_{-\infty}^{x} \frac{1}{\sqrt{2\pi}} \exp(-\frac{x^2}{2})dx \tag{55}$$

is a cumulative error function. From this, we easily find that when output SNR equals h, which is a threshold parameter, detection probability is 50 %. **Figure 9** shows detection probability in a stationary state of RMF calculated by (54). Here we set $h = 7.5$. From this figure, we find that when $\nu = 3 \times 3$ and $\nu = 7 \times 7$ it is sufficient that input SNR is greater than 2.6 and 3.2, respectively, for target detection with probability of 90%.

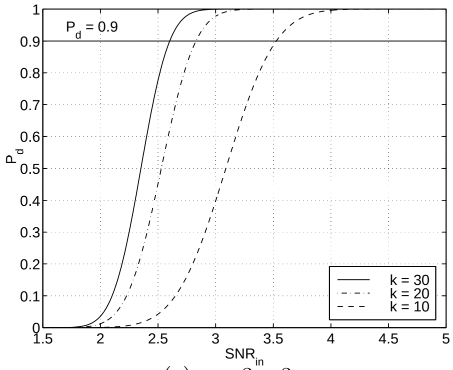

(a) $\nu = 3 \times 3$

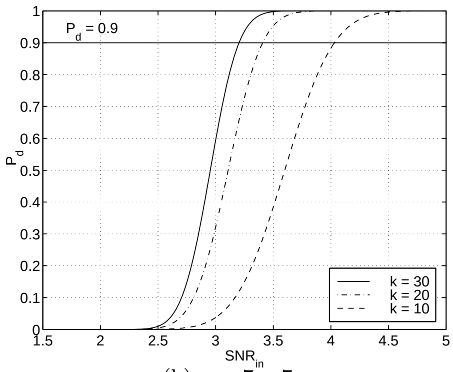

(b) $\nu = 7 \times 7$

Fig. 9 Detection probability

6. Conclusion

We formulated RMF, which was previously proposed as an image processing algorithm for the detection of small moving targets, from a Bayesian viewpoint and showed that it could be interpreted as a Bellman equation of DP.

We also derived approximate expressions to describe the distribution of RMF outputs and used them to analyze RMF performance. In performance analysis, first, we showed that output SNR can be increased indefinitely, if input SNR is greater than a certain value, and we obtained the values of the limit SNR. Next, we obtained the false alarm and detection probabilities with the aid of simulation and approximate expressions and clarified the condition under which targets were detectable.

Though we clarified the fundamental features of RMF assuming that the background noise is white and Gaussian, there are many applications where this assumption is not satisfied at the outset. In these applications, some preprocessing will be required before applying RMF, which is a future task for expanding applications.

References

1) Y. Barniv, "Dynamic programming solution for detecting dim moving targets," IEEE Transactions on Aerospace and Electronic Systems, **21**-1, 144/156 (1985)
2) N. C. Mohanty, "Computer tracking of moving point targets in space," *IEEE Trans. Pattern Anal. Machine Intell.,* vol. PAMI-3, no. 5, 606/611 (1981)
3) I. S. Reed, R. M. Gagliardi, and H. M. Shao, "Application of three-dimensional filtering to moving target detection," *IEEE Transactions on Aerospace and Electronic Systems,* vol. AES-19, Nov., 898/905 (1983)
4) I. S. Reed, R. M. Gagliardi, and L. Stotts, "Optical moving target detection with 3-D matched filtering," *IEEE Transactions on Aerospace and Electronic Systems,* vol. AES-24, July., 327/336 (1988)
5) J. Arnold, S. Shaw and H. Pasternack, "Efficient target tracking using dynamic programming," IEEE Trans. AES, vol. 29, no. 1, Jan, 44/56 (1993)
6) Y. Barniv and O. Kella, "Dynamic programming solution for detecting dim moving targets, Part II: Analysis," IEEE Transactions on Aerospace and Electronic Systems, **23**-4, 776/788 (1987)
7) S. M. Tonissen and R. J. Evans, "Performance of dynamic programming techniques for track-before-detect," IEEE Transactions on Aerospace and Electronic Systems, **32**-4, 1440/1451 (1996)
8) L. Johnston and V. Krishnamurthy, "Performance analysis of a dynamic programming track before detect algorithm," IEEE Transactions on Aerospace and Electronic Systems, **38**-1, 228/242 (2002)
9) K. Nishiguchi et al., "Small target detection from image sequences using recursive max filter," SPIE Conference on Signal and Data Processing for Small Targets 1995, **2561**, 153/166 (1995)
10) K. Nishiguchi and S. Yoshikawa: Dim star detection for star sensor using recursive maximum filte," Trans. of the SICE, **40**-5, 573/582 (2004) (in Japanese)
11) K. Nishiguchi and S. Yoshikawa: Star detection method for star sensor images using recursive maximum filter, 24th International Symposium on Space Technology and Science (ISTS2004), Miyazaki, Japan, (2004)
12) G. L. Tietjen, D. K. Kahaner and R. J. Beckman, "Variances and covariances of the normal order statistics for sample sizes 2 to 50,"in *Selected Tables in Mathematical Statistics, Volume V*, pp.1–73, American Mathematical Society, 197

Appendix A. Approximation of the mean of output noise

In this appendix, we derive (22), which is an approximation expression of the mean of output noise. In preparation, we define the local mean and local variance by

$$\overline{X}_{ij}(k) = \frac{1}{\nu} \sum_{(i',j') \in D_{ij}} X_{i'j'}(k), \tag{A. 1}$$

$$V_{X,ij}(k) = \frac{1}{\nu - 1} \sum_{(i',j') \in D_{ij}} (X_{i'j'}(k) - \overline{X}_{ij}(k))^2, \tag{A. 2}$$

respectively, and represent the expectation of the local variance as

$$\sigma^2_{X,\mathrm{loc}}(k) = EV_{X,ij}(k) \tag{A. 3}$$

where coefficient $1/(\nu-1)$ of (A. 2) is determined so that if $\{X_{ij}(k)\}$ are i.i.d. in neighborhood D_{ij}, then $\sigma^2_{X,\mathrm{loc}}(k)$ equals the variance of $\{X_{ij}(k)\}$.

Now, let $X_1, X_2, \cdots, X_\nu$ be i.i.d. normal variables with mean μ_X and variance σ_X^2, and we define the sample maximum by

$$Z = \max_{i=1,\cdots,\nu} X_i, \tag{A. 4}$$

and then the mean and the variance of Z are given by

$$EZ = \mu_X + \mu_{(\nu)}\sigma_X, \tag{A. 5}$$

$$E(Z - EZ)^2 = \sigma^2_{(\nu)}\sigma^2_X. \tag{A. 6}$$

To derive approximation expressions, we assume similar relations with respect to output noise and its local maximum defined by (25) as:

Assumption 1.

$$EZ_{ij}(k) \;=\; \mu_{\mathrm{out}}(k) + \mu_{(\nu)}\sigma_{X,\mathrm{loc}}(k) \tag{A. 7}$$

$$\sigma^2_{Z,\mathrm{loc}}(k) \;=\; \sigma^2_{(\nu)}\sigma^2_{X,\mathrm{loc}}(k) \tag{A. 8}$$

where $\mu_{\mathrm{out}}(k) = EX_{ij}(k)$, and $\sigma^2_{Z,\mathrm{loc}}(k)$ is the expectation of the local variance of $\{Z_{ij}(k)\}$. Assumption 1 holds exactly when $\{X_{i'j'}(k)\}_{(i',j')\in D_{i,j}}$ are i.i.d. normal variables.

Under assumption 1, the expectations of $X_{ij}(k)$ and of the local variance of $X_{ij}(k)$ follow the recursive formula:

$$\mu_{\mathrm{out}}(k) \;=\; \alpha\left[\mu_{\mathrm{out}}(k-1) + \mu_{(\nu)}\sigma_{X,\mathrm{loc}}(k-1)\right], \tag{A. 9}$$

$$\sigma^2_{X,\mathrm{loc}}(k) \;=\; 1 + \alpha^2\sigma^2_{(\nu)}\sigma^2_{X,\mathrm{loc}}(k-1), \tag{A. 10}$$

which can be solved explicitly under the initial condition $\mu_{\mathrm{out}}(1) = 0$ and $\sigma^2_{X,\mathrm{loc}}(1) = 1$, so we have

$$\mu_{\mathrm{out}}(k) \;=\; \mu_{(\nu)}\sum_{l=1}^{k-1}\alpha^l\sigma_{X,\mathrm{loc}}(l), \tag{A. 11}$$

$$\sigma^2_{X,\mathrm{loc}}(k) \;=\; \frac{1-(\alpha\sigma_{(\nu)})^{2k}}{1-(\alpha\sigma_{(\nu)})^2}. \tag{A. 12}$$

When k increases, local variance is saturated and becomes

$$\sigma^2_{X,\mathrm{loc}}(k) \sim \frac{1}{1-(\alpha\sigma_{(\nu)})^2} \tag{A. 13}$$

, and the mean becomes

$$\mu_{\mathrm{out}}(k) \sim \begin{cases} \alpha\dfrac{1-\alpha^{k-1}}{1-\alpha}\mu_0(\nu,\alpha), & \alpha < 1 \\ (k-1)\mu_0(\nu,1), & \alpha = 1 \end{cases} \tag{A. 14}$$

where $\mu_0(\nu,\alpha)$ is the variable defined by (23).

Ken'ichi Nishiguchi (Member)

He received a B.S. degree in mathematics from Kyoto University in 1974 and a Ph.D. degree in engineering from Osaka University in 1994. In 1974 he joined Mitsubishi Electric Corporation's Central Research Laboratory (reorganized as the Advanced Technology R&D Center). Since 2007, he has been a specially appointed professor at Osaka University. His research interests include modeling and the analysis of stochastic systems, statistical signal and image processing, and nonlinear optics.

Reprinted from Trans. of the SICE
Vol. 41 No. 7 603/611 2005